Commercial CMOS image sensors as X-ray imagers and particle beam monitors

A. Castoldi,[a,b,1] **C. Guazzoni,**[a,b] **S. Maffessanti,**[a] **G.V. Montemurro**[a] **and L. Carraresi**[c,d]

[a] *Politecnico di Milano, Dip. Elettronica, Informazione e Bioingegneria, Piazza Leonardo da Vinci 32, 20133 Milano, Italy*

[b] *INFN, Sezione di Milano, Via Celoria 16, 20133 Milano, Italy*

[c] *Università degli Studi di Firenze, Dip. Fisica e Astronomia, Via G. Sansone 1, 50019 Sesto Fiorentino (FI)*

[d] *INFN, Sezione di Firenze, Via, G. Sansone 1, 50019 Sesto Fiorentino (FI), Italy*

E-mail: Andrea.Castoldi@polimi.it

1 Introduction

CMOS image sensors are widely used in several applications such as mobile handsets webcams and digital cameras among others. Furthermore they are available across a wide range of resolutions with excellent spectral and chromatic responses.

In order to fulfil the need of cheap and high-resolution systems as radiation beam monitors we exploited the possibility of using commercial CMOS image sensors as X-ray and low-intensity particle beam monitors. The generally low cost of the sensors make it possible to alleviate the issue of radiation damage and consider the sensor somehow to be disposable after a given time.

A first CMOS sensor featuring 752×480 pixels, $6\ \mu\text{m} \times 6\ \mu\text{m}$ pixel size, has been mounted and successfully tested as bi-dimensional beam profile monitor at the pulsed proton beamline DeFEL (1–6 MeV pulsed proton beam) of the LaBeC of INFN in Florence. The naked sensor is able to take snapshots of the incoming proton bunches and, in particular, to detect the interactions of the single protons.

A second CMOS sensor, featuring 1472×1096 pixels, $2.2 \times 2.2\ \mu\text{m}$ pixel size, has been mounted on a dedicated board as high-resolution X-ray imager in X-ray imaging experiments with table-top X-ray generators.

This paper focuses on the description of the architecture of the sensor systems and on the results of the experimental measurements.

[1] Corresponding author.

2 Pulsed proton beam 2D monitor

The first developed system is intended to act as beam monitor at the pulsed mono-energetic proton beamline DeFEL of the 3 MV Tandetron accelerator located at LaBeC (Laboratorio di tecniche nucleari per i Beni Culturali) of INFN in Florence, Italy [1].

At DeFEL the continuous beam coming from the accelerator is deflected transversally across a slit allowing a bunch of protons (or ions) to proceed downstream through an aperture only during a very short time interval of the order of 1 ns. The adjustment of the size of the aperture with a motorized slit, and of the intensity of the continuous beam, is the key feature to create a pulsed beam with a variable and finely controllable number of particles in each pulse (down to an average value much below 1 proton per trigger and with a position of interaction in a defined area of down to better than 40 μm $\times$ 40 μm). The DeFEL beamline is able to provide bunches of protons with tunable energies in the range from 1 up to 6 MeV which is suitable for the qualification, diagnostics and calibration of radiation detectors at high ionization levels.

2.1 CMOS sensor and experimental setup

A CMOS sensor (Aptina MT9v034) featuring 752 $\times$ 480 pixels, 6 μm $\times$ 6 μm pixel size, has been mounted as 2D beam profile monitor The CMOS camera must work in vacuum inside the experimental chamber to allow precise monitoring of the proton beam cross-section and of the bunch multiplicity.

The Aptina sensor is connected to the video interface of a Beagle board (xM), ARM 37x 1GHz by means of a 12 bits data bus and by means of I2C connection for programming the registers of the slow camera controls. The number of pixels, the choice of the readout mode and all the register settings are defined in specific modules of the Linux kernel. Some of the relevant parameters, e.g. integration time and the possibility to reduce resolution (1/4 or 1/9 of the native resolution), can be defined at execution time.

Single frames can be read as binary files and stored locally (e.g. on SD card) or transferred via ethernet to a host PC outside the vacuum for further post-processing. The number of frame per second depends on the size of the CMOS sensor and on the storage medium: from 5–10 fps for a 748 $\times$ 480 pixel image stored on SD card to less than 1 fps for a 2500 $\times$ 1900 pixel image transferred via ethernet. Despite the limited frame rate, such performance is adequate as beam monitor at the DeFEL beamline where the bunch repetition rate is normally limited to less than few kHz.

Figure 1 shows the photograph of the CMOS sensor setup for operation in vacuum in the DeFEL experimental chamber. The Aptina MT9v034 sensor is mounted directly on the Beagle board coupled to a custom Copper block and a cooling structure specifically developed for operation in vacuum.

2.2 Qualification of the CMOS sensor Point Spread Function

In order to evaluate the performance of the CMOS sensor as beam monitor we qualified the sensor Point Spread Function. To this aim the detector was directly irradiated with 1 MeV protons impinging at 0 $^\circ$ on the CMOS sensor, placed in the DeFEL vacuum chamber. A single 1 MeV proton

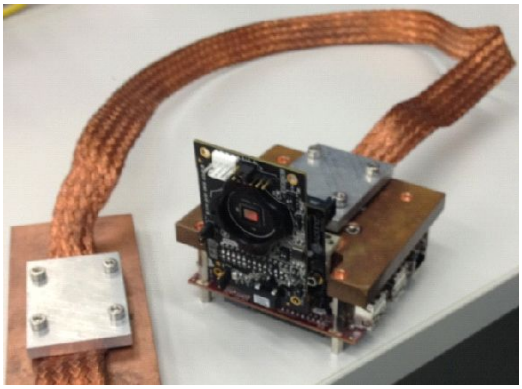

Figure 1. Photograph of the CMOS sensor setup for operation in vacuum in the DeFEL experimental chamber.

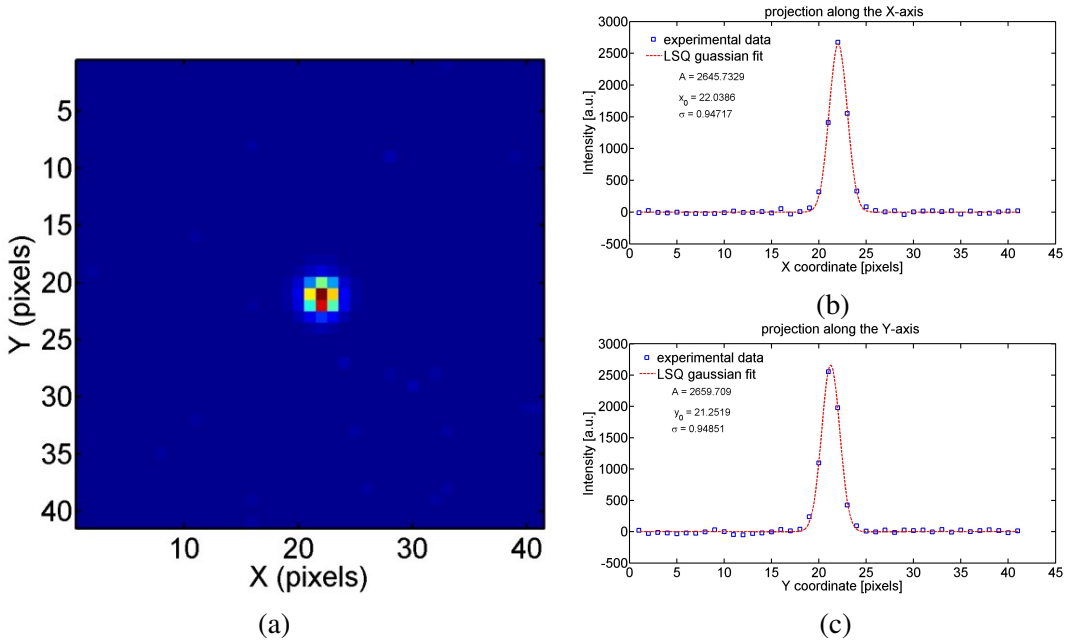

(a) (b) (c)

Figure 2. (a) Image of a single 1 MeV proton detection. (b) Projection along the X-axis. (c) Projection along the Y-axis. The PSF in both directions is about 1 pixel r.m.s., as derived from the Gaussian fit.

— fully absorbed in Silicon — generates 277,780 electrons/holes pairs. Figure 2 shows the typical image of a single 1 MeV proton detection, as acquired with the CMOS sensor. By projecting the image along the Cartesian axes, and Least-Square fitting the experimental data, we derived the Point Spread Function of the sensor that turns out to be about 1 pixel r.m.s. in both directions in the case of 1 MeV protons.

2.3 Application of the CMOS sensor for beam tuning

The CMOS sensor has been used to check the beam cross-section as a function of the nominal dimensions set on the extraction slits. For relatively large values of the set dimensions a perfect match is achieved. Shrinking the slits opening does not shrink the beam profile accordingly.

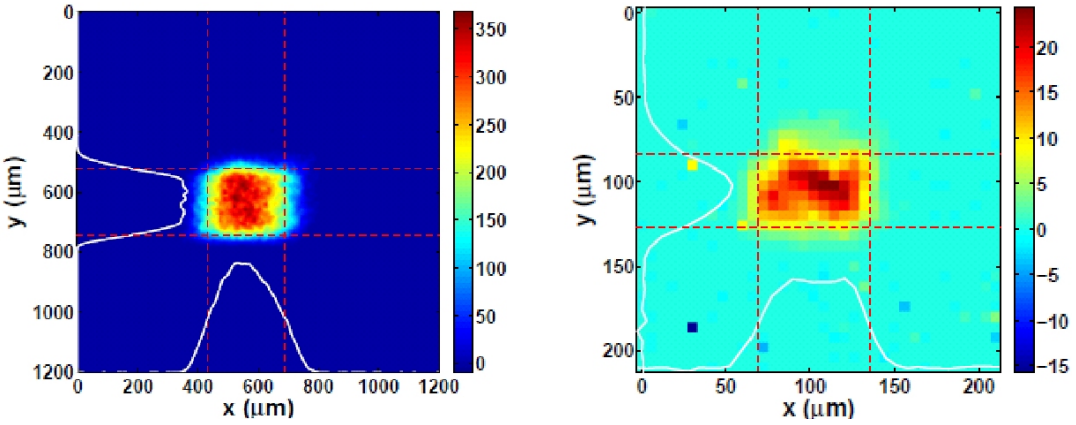

Figure 3. Two-dimensional beam cross-section of the proton beam: (a) 200 μm $\times$ 200 μm nominal opening of the final slits, quadrupole currents Q1=Q2=2 A. The white lines are the 1D projections along the x and y axes, while the red dashed lines define the FWHM size of the profile, that is 254 um $\times$ 220 um . (b) 30 μm $\times$ 30 μm nominal opening of the final slits, quadrupole currents Q1=Q2=1.4 A. The white lines are the 1D projections along the x and y axes, while the red dashed lines define the FWHM size of the profile, that is 65 um $\times$ 42 um.

Recently we upgraded the DeFEL beam line performance in terms of spatial resolution of the proton beam with novel remotely controlled in-vacuum hi-resolution profiling slits with the aim to reduce the proton beam cross-section in the end station [2]. Since the focusing of the beam in the two transversal directions can be adjusted by two quadrupoles along the beam line, the developed CMOS sensor system has been used to monitor the tuning of the beam profile.

The spatial properties of the proton beam have been qualified by directly irradiating the installed CMOS imager with 1 MeV protons. The 2D beam profile is obtained by adding a sufficient number of single exposure frames and normalizing to the number of frames. Dark-frame subtraction on every frame has been applied to minimize image noise (fix pattern noise from the sensor, dead or hot pixels). Figure 3 shows a two-dimensional profile of the proton beam collected with the CMOS sensor. The DeFEL trigger frequency (proton bunches repetition rate) was 500 Hz and the CMOS exposure time was set to 62.5 ms, a total of 1024 frames has been acquired. Images were dark-frame subtracted and summed to get a better statistics. The colorbar gives the intensity of the beam impinging during total exposure time. The 2D profile can then be projected onto the x and y axes and the mono-dimensional profiles analyzed to evaluate the full width half maximum (FWHM) of the beam in both directions. The computation of the FWHM has been performed by considering a threshold at half between the maximum and minimum values of the mono-dimensional profile. The threshold crossing spatial coordinate is achieved with a linear interpolation of the mono-dimensional profile values immediately under and above the threshold. The measured 2D beam profile shows a slight discrepancy with respect to the nominal opening of the profiling slits related to the sub-optimal focusing of the quadrupoles.

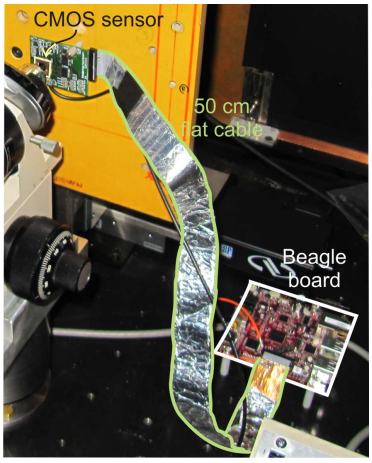

Figure 4. Photograph of the CMOS sensor setup for operation as beam monitor in the lab-based X-ray imaging suite. The main system components are highlighted.

3 X-ray beam monitor

The second system under development is intended to act as beam qualification monitor in a lab-based imaging system aimed at X-ray fluorescence imaging [3] and X-ray scatter imaging [4], based on a collimated X-ray generator (X-Beam Powerflux PC from X-ray Optical Systems, Inc, Mo anode, 50 kV high voltage) equipped with a polycapillary collimator and on high resolution energy dispersive detectors based on the side-ward depletion principle.

3.1 CMOS sensor and experimental setup

The chosen sensor is an Aptina MT9M032 featuring 1472 $\times$ 1096 pixels, 2.2 $\times$ 2.2 μm pixel size. The nominal Silicon thickness — as declared in the datasheet — is 305 μm, while no estimation of the active (depleted) region is available. The mounting of the CMOS imager on a compact dedicated board — custom designed and equipped with the needed transceivers — allows an easy placement of the beam monitor during X-ray imaging experiments while the digital board is several tens of centimetres apart. In order to simplify data transfer and image acquisition, the system is controlled by a dedicated micro-processor board (DM3730 1GHz SoC ARM Cortex-A8) on which a modified LINUX kernel has been implemented. Figure 4 shows the photograph of the CMOS sensor setup for operation as beam monitor in the lab-based X-ray imaging suite.

3.2 Use as X-ray beam monitor

The CMOS sensor has been mounted close to the beam collimator slits, as shown in figure 5, to monitor the 2D beam profile as a function of the distance from the beam profiling slits and therefore to assess the beam quality.

Figure 6 shows the acquired images at two different distances, one very close to the collimating slits (3.29 cm) and the second at farther distance (39.24 cm) for different openings of the profiling slits (1 mm $\times$ 1 mm, 0.5 mm $\times$ 0.5 mm, 0.2 mm $\times$ 0.2 mm, 0.1 mm $\times$ 0.1 mm). Despite the limited efficiency of the sensor due to the small depleted volume — whose thickness is not known and

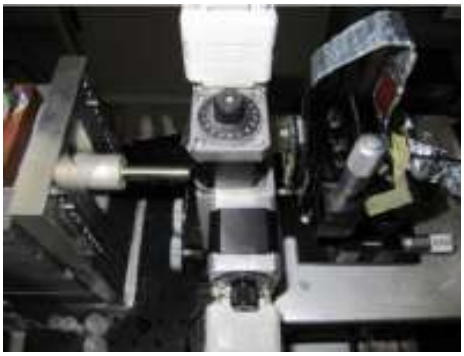

Figure 5. Detail of the CMOS imager mounted after the beam collimator slits (at a distance of 3.29 cm) to monitor the X-ray beam profile.

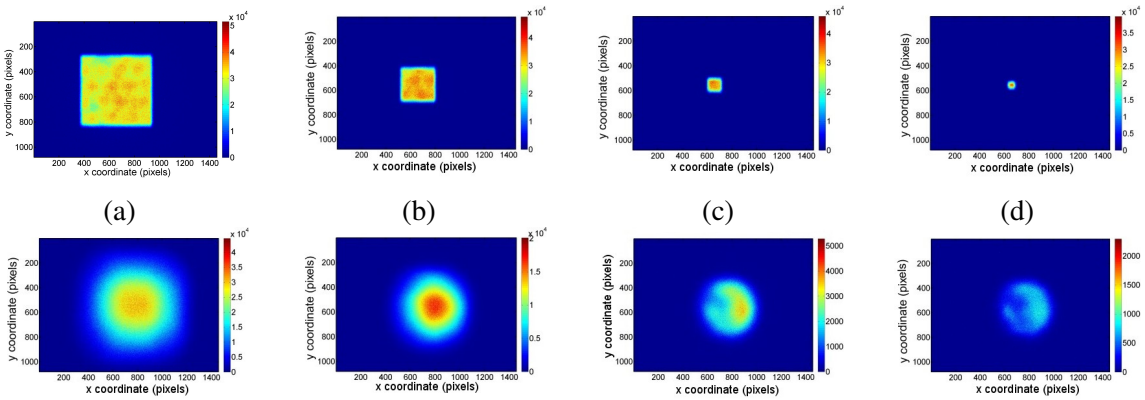

Figure 6. Two-dimensional beam cross-section of the X-ray beam (a, b, c, d, e X-ray generator set to 50 kV, 0.4 mA; f, g, h X-ray generator set to 50 kV, 1 mA) for different openings of the profiling slits (1 mm, 0.5 mm, 0.2 mm, 0.1 mm) and for two different distances along the beam (a, b, c, d 3.29 cm) (e, f, g, h 39.24 cm). Images were normalized to 0.4 mA beam current. The non-uniformity of the beam - related to the polycapillary lens - and the beam divergence can be clearly seen. The colorbar represents arbitrary units, with a scale common to all sub-figures.

cannot be easily quantified — the quality of the images is pretty good and allows studying the beam profile as required by the aforementioned application in X-ray fluorescence and X-ray diffraction imaging. In order to get a better insight of the beam quality we studied also the 1D beam profile, shown in figure 7. The acquired images allowed the qualification of the beam transverse divergence and highlighted the non-uniformity of the beam — related to the collimating polycapillary lens coupled to the X-ray generator. Table 1 shows the FWHM extracted from the measured profiles at the closer distance.

3.3 High-resolution X-ray micro-imaging

We investigated the possibility of applying the CMOS sensor in X-ray micro-imaging of small objects. Figure 8 shows the pseudo-colour micro-images of a mini bulb lamp (Mag-Lite LM3A001) and of a M09 screw. In both cases the X-ray generator was set to 50 kV terminal voltage and 0.4 mA

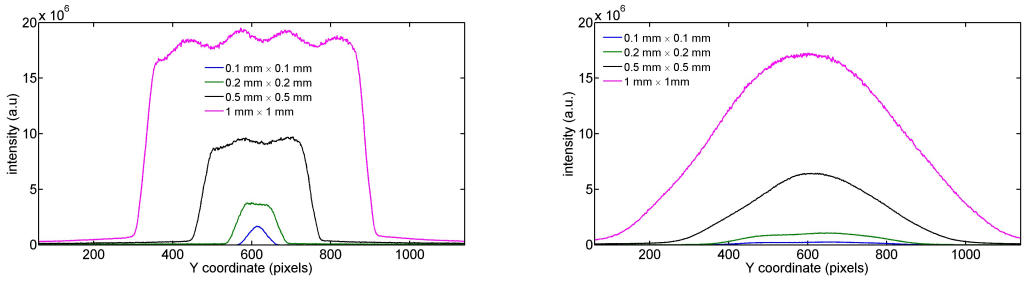

Figure 7. 1-D profile along the Y coordinate for the different openings of the profiling slits at the same distances shown in figure 6. In the left image (distance 3.29 cm), the undulations of the profile show clearly the non-uniformity of the beam related to the polycapillary lens.

Table 1. Measured FWHM along y coordinate vs slit opening.

Slits opening (mm)	**FWHM along y coordinate (μm)**
1	1214
0.5	598
0.2	233
0.1	110

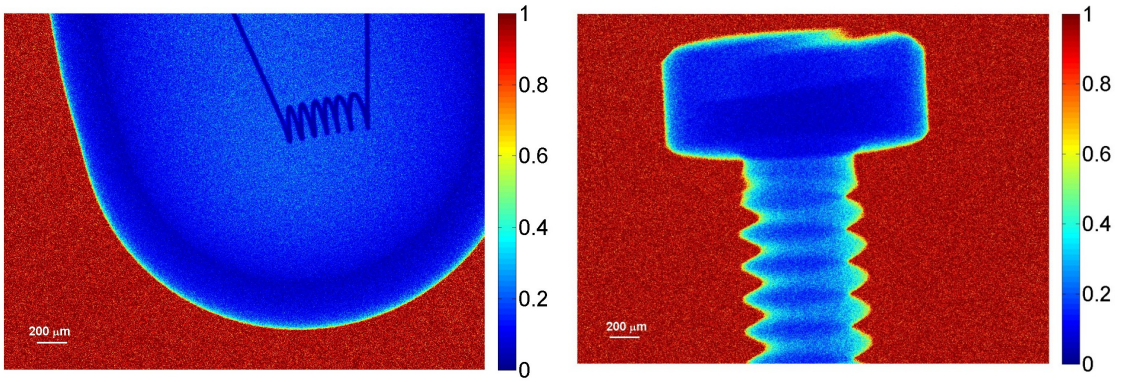

(a) (b)

Figure 8. X-ray transmission micro-imaging of small objects. (a) mini bulb lamp (Mag-Lite LM3A001) (50 kV, 0.4 mA). The filament diameter is about 25 μm. (b) M09 screw (50 kV, 0.4 mA). Both images have been dark-image subtracted and normalized to the dark-subtracted flat-field image.

beam current. Both objects feature small details of few tens of micrometers that are beautifully visible in the images.

4 Conclusions

In order to fulfill the need of cheap systems as beam monitors and high resolution image sensors we exploited the possibility of using commercial CMOS image sensors as X-rays and proton detectors. Two different sensors have been mounted and tested, both from Aptina. The sensors have been mounted in dedicated setups and succesfully applied both as bi-dimensional beam profile monitor,

able to take pictures of the incoming proton bunches at the DeFEL beamline (1–6 MeV pulsed proton beam) of the LaBeC of INFN in Florence and as high-resolution X-ray micro-imager to qualify the beam profile from table-top generators used in advanced imaging modality setups.

References

[1] F.A. Mirto and L. Carraresi, *The pulsed beam facility at the Tandetron accelerator in Florence*, *Nucl. Instrum. Meth.* **B 266** (2008) 2113.

[2] A. Castoldi et al., *Upgrade of the DeFEL Proton Beamline for Detector Response Mapping*, *IEEE Nucl. Sci. Symp. Med. Imag. Conf. Rec.* (2013) 1.

[3] K. Ricketts et al., *An x-ray fluorescence imaging system for gold nanoparticle detection*, *Phys. Med. Biol.* **58** (2013) 7841.

[4] A. Castoldi et al., *Experimental Qualification of a Novel X-ray Diffraction Imaging Setup Based on Polycapillary X-ray Optics*, *IEEE Trans. Nucl. Sci.* **57** (2010) 2564.